LIMNOLOGY and OCEANOGRAPHY

ASLO

Limnol. Oceanogr. 67, 2022, 1522–1536

doi: 10.1002/lno.12099

Water chemistry variation in tropical high-mountain lakes on old volcanic bedrocks

Pablo V. Mosquera [1,2] **Henrietta Hampel** [3] **Raúl F. Vázquez** [4] **Jordi Catalan** [5,6*]

[1]Departament de Biologia Evolutiva, Ecologia i Ciències Ambientals, Universitat de Barcelona, Barcelona, Spain
[2]Subgerencia de Gestión Ambiental de la Empresa Pública Municipal de Telecomunicaciones, Agua potable, Alcantarillado y Saneamiento (ETAPA EP), Cuenca, Ecuador
[3]Laboratorio de Ecología Acuática, Facultad de Ciencias Químicas, Universidad de Cuenca, Cuenca, Ecuador
[4]Departamento de Ingeniería Civil, Facultad de Ingeniería, Universidad de Cuenca, Cuenca, Ecuador
[5]CREAF, Cerdanyola del Vallès, Spain
[6]CSIC, Cerdanyola del Vallès, Spain

Abstract

Water chemistry and its ecological implications have been extensively investigated in temperate high-mountain lakes because of their role as sentinels of global change. However, few studies have considered the drivers of water chemistry in tropical mountain lakes underlain by volcanic bedrock. A survey of 165 páramo lakes in the Cajas Massif of the Southern Ecuador Andes identified 4 independent chemical variation gradients, primarily characterized by divalent cations (hardness), organic carbon, silica, and iron levels. Hardness and silica factors showed contrasting relationships with parent rock type and age, vegetation, aquatic ecosystems in the watershed, and lake and watershed size. Geochemical considerations suggest that divalent cations (and related alkalinity, conductivity, and pH) mainly respond to the cumulative partial dissolution of primary aluminosilicates distributed throughout the subsurface of watersheds, and silica and monovalent cations are associated with the congruent dissolution of large amounts of secondary aluminosilicates localized in former hydrothermal or tectonic spots. Dissolved organic carbon was much higher than in temperate high-mountain lakes, causing extra acidity in water. The smaller the lakes and their watersheds, the higher the likelihood of elevated organic carbon and metals and low hardness. The watershed wetland cover favored metal levels in the lakes but not organic carbon. Phosphorus, positively, and nitrate, negatively, weakly correlated with the metal gradient, indicating common influence by in-lake processes. Overall, the study revealed that relatively small tropical lake districts on volcanic basins can show chemical variation equivalent to that in large mountain ranges with a combination of plutonic, metamorphic, and carbonate rock areas.

Orogenesis provides crystalline bedrock with low permeability and, consequently, past glacial excavation promoted lake districts on many high mountains around the world (Jacobsen and Dangles 2017). The water chemical composition of these lakes is driven by atmospheric deposition, geological background, watershed and in-lake biological activity, and human influence (Psenner and Catalan 1994). Crystalline rocks usually lack readily soluble minerals; therefore, lakes and headwaters in mountains show low salt content and low acid-neutralizing capacity, making them sensitive to acidic deposition. As a consequence of the "Great acceleration" (Steffen et al. 2015), emissions of sulfur and nitrogen oxides to the atmosphere caused the acidification of ecosystems in remote areas, including mountains in North America (Beamish and Harvey 1972) and Europe (Massabuau et al. 1987). High-mountain lakes became indicators of the acidification process and its ecological impact (Kopáček et al. 1998; Rogora et al. 2001). Interest in the biogeochemistry and biota of mountain lakes has increased, and as a result, information and knowledge have been accumulating over the last decades (Catalan et al. 2009*b*). Currently, high-mountain lakes across the globe are considered sentinels of the systemic change of

*Correspondence: j.catalan@creaf.uab.cat

Additional Supporting Information may be found in the online version of this article.

Author Contribution Statement: P.V.M., H.H. and R.F.V. planned the lake survey and provided financial support. P.V.M. performed field sampling, coordinated chemical analyses, and developed the land cover map. P.V.M. and R.F.V. performed GIS analyses and developed the land class mapping. J.C. and P.V.M. performed the data analyses, outlined the manuscript, and wrote the initial draft. All authors provided valuable discussion points and revisions to the manuscript.

the planet (Moser et al. 2019). In this context, there is a growing interest in tropical high-mountain lakes (Michelutti et al. 2015; Van Colen et al. 2017; Benito et al. 2019; Steinitz-Kannan et al. 2020; Zapata et al. 2021), which have historically received less attention (Eggermont et al. 2007). Although high-mountain lakes are among the most comparable ecosystems globally, and a common conceptual framework might be used to analyze them (Catalan and Donato-Rondón 2016), tropical high-mountain lake regions have unique environmental characteristics that require special attention. Seasonal weather changes are low, and mean air temperature and rainfall are higher than in temperate high-mountain lake districts (Jacobsen and Dangles 2017).

The chemical composition of water in temperate high-mountain lake districts is primarily related to the bedrock (Psenner 1989; Nauwerck 1994; Marchetto et al. 1995; Kamenik et al. 2001). Although the ionic strength is consistently lower than that of low-land waters, temperate mountain lakes on metamorphic, plutonic, or carbonate rocks may markedly vary in acidity and dominant ions under similar sea salt- and human-influenced atmospheric deposition (Catalan et al. 1993). Mountain lake districts that show considerable chemical variation usually have a high diversity of bedrock composition, common in large massifs and ranges resulting from old collisional orogeny (Camarero et al. 2009). Uplifted and bent sedimentary rock landscapes may include highly metamorphosed materials, which eventually surround intrusive igneous rocks. Slates rich in sulfides may provide highly acidic waters, granitic batholiths have very low ionic levels, whereas carbonate bedrock holds alkaline waters (Marchetto et al. 1995). This broad range of chemical conditions provides niche gradients for species segregation (Catalan et al. 2009*a*).

Many tropical lake districts are located on volcanic bedrock in young accretionary orogenic belts. Therefore, the chemical diversity that results from weathering could be expected to be lower than in the ranges of high lithologic diversity. Furthermore, alpine areas in temperate zones continuously expose fresh rock to chemical weathering, fostered by cryofracturing of bare rock and unstable slopes. In tropical zones, warmer conditions and high vegetation cover likely diminish the availability of exposed surfaces, with rock weathering relegated to deep subsoils. Soils in tropical high-mountain lake districts have a postglacial origin. Despite their relatively young origin, they are depleted in exchangeable cations because of the high rainfall and relatively warm temperature (Molina et al. 2019). Therefore, we might expect less chemical diversity and lower acid-neutralizing capacity in mountain lakes on tropical volcanic bedrock than in temperate mountain lake districts. However, the limited data available suggests that significant variation may occur (Armienta et al. 2008; Catalan and Donato-Rondón 2016), perhaps related to the higher weatherability of basaltic lithologies compared to granite (Dupre et al. 2003), which may result in higher temporal and spatial heterogeneity of the process over the same substrate.

Consequently, this study aimed to comprehensively analyze the primary drivers of water chemistry variation in a tropical lake district on volcanic bedrock. We performed an extensive survey of the lakes and ponds ($n = 165$) in the Cajas Massif in the Andes of Southern Ecuador and measured the main chemical components of surface waters. The chemical variation was related to lake and watershed morphological characteristics, volcanic geological formations, and land cover. We evaluated the possible mechanisms behind the observed patterns concerning rock weathering in the spatially complex lithology provided by volcanism and a water-saturated cold tropical landscape that fosters organic matter accumulation. Finally, we briefly discuss the potential ecological implications of the chemical variation for constraints and ecological thresholds in species distributions and metacommunity dynamics.

Material and methods

Study sites and sampling

The Cajas Massif in the Southern Ecuador Andes contains approximately 6000 lakes and ponds of glacial origin (Mosquera et al. 2017*a*). The present study included data from 165 water bodies (Fig. 1), mainly within the Cajas National Park (CNP). Lakes (> 0.5 ha) were selected proportionally to their density in the 2 main hydrological basins of the CNP (western, eastern) and 15 subbasins (Supporting Information Fig. S1). Two other watersheds outside the park were also included to consider the lakes at the highest altitudes. In each subbasin, we sampled the largest lakes and a proportion of the rest (> 50%) based on altitude and size distribution (Table 1). When visiting the lakes, ponds were opportunistically sampled by heuristically selecting those of varying characteristics (e.g., transparency, macrophyte cover). Lake bathymetries are available from all water bodies (Mosquera et al. 2017*a*). Although the area studied was relatively small (~ 334 km^2), it represented the entire Cajas Massif variation in lithology, vegetation, and aquatic ecosystems. The landscape corresponds to páramo ecosystems with surplus water (Carrillo-Rojas et al. 2016). Seasonal and interannual rainfall modes correspond to the equatorial Andes (5°S–1°N), characterized by a bimodal regime with wet periods from February to April and October to November associated with a westward humidity transport from the equatorial Amazon (Segura et al. 2019) with occasional extreme fluctuations conditioned by the equatorial Pacific (Oñate-Valdivieso et al. 2018; Schneider et al. 2018). Although the Amazonian air masses tend to lose humidity over the eastern flanks of the cordillera, rainfall occurs throughout the year (only ~ 12% dry days) at the lake district elevation, primarily as drizzle (~ 80% duration), with mean annual precipitation in the Cajas Massif from ca. 900–1400 mm, with the maximum around 3400 m a.s.l. (Padrón et al. 2015). Cloud condensation is common, and fog interception can increase conventional rainfall by > 25% (Rollenbeck et al. 2011).

A lake survey for chemical analysis was carried out during 2014–2015. Lakes with > 1-m depth (76%) were sampled at

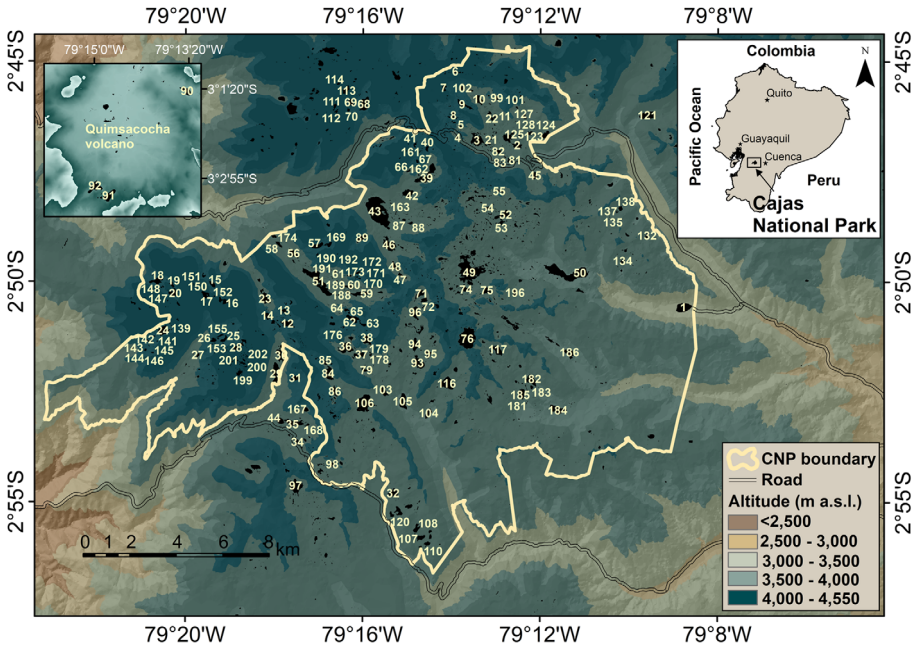

Fig. 1. Location of the study area and lakes. The large majority are located in the Cajas National Park (162), and some are in the Quimsacocha volcano area (3) and Sangay National Park (Culebrillas lake, #157, not shown). Identifiers correspond to codes from Mosquera et al. (2017*b*).

Table 1. Summary of the physical features of 165 lakes and ponds sampled for this study.

Variable	Unit	Minimum	First quartile	Median	Mean	Third quartile	Maximum
Latitude, N	Degrees	−3.05	−2.86	−2.84	−2.83	−2.80	−2.42
Longitude, E	Degrees	−79.35	−79.29	−79.26	−79.26	−79.23	−78.86
Altitude	m a.s.l.	3152	3856	3958	3945	4043	4294
Maximum depth	m	0.15	1.50	8.25	13	18	76
Mean depth	m	0.05	0.50	2.5	4.8	6.6	30.6
Area	m^2	22	12,177	32,012	68,698	81,331	774,775
Volume	m^3	3.2	6214	72,124	841,645	521,336	22,369,167
Watershed area	km^2	0.00002	0.28	0.98	2.74	2.19	47.70

the deepest point from a dinghy; shallower lakes and ponds were sampled from the shoreline. The upper mixed layer was determined by performing temperature profiles, and water samples were collected using Van Dorn bottles (3 L) every two meters and integrated. Water samples were immediately screened (64-μm mesh) to remove zooplankton and debris before being cold stored and transported to ETAPA EP labs in the nearby city of Cuenca (Ecuador) for analysis. For nitrate, soluble reactive phosphorus (SRP) and dissolved organic carbon (DOC) samples were filtered using precombusted (450 °C, 4 h) GF/F Whatman® (Maidstone) 47-mm Ø glass fiber filters and Swinnex® (Merck Millipore) syringes.

Chemical analysis

Standard methods for water chemical analyses were followed (APHA-AWWA-WEF 2012). Sodium, potassium, silica, aluminum (only for 2019–2020 samples), iron, and manganese were determined by inductively coupled plasma spectrometry (SM 3120 B; ICP-OES, Optima 7000 DV, PerkinElmer); calcium and magnesium by ethylenediaminetetraacetic acid (EDTA) titrimetric methods (SM 3500-Ca B and 3500-Mg B); alkalinity by potentiometric titration (SM 2320Bb); sulfate by a turbidimetric method (SM 4500 SO_4^{2-} E); chloride by mercuric nitrate titration (SM 4500-Cl^- C); SRP and total phosphorus (TP) following the method of Murphy and Riley (1962), the latter after potassium persulfate digestion; nitrate was reduced to nitrite and determined by colorimetry (SM 4500-NO_3^- E); ammonium by the salicylate method (10012, HACH), total organic carbon (TOC), and DOC by acidic digestion (Method 10129, HACH). Conductivity at 20°C was measured using a YSI-EXO-1 sensor and pH with a WTW 3320 pH meter (Xylem Analytics) equipped with a sensor for low-ionic-strength samples (SenTix® HW). Apparent color was determined spectrophotometrically using platinum–cobalt standards (SM 2120 C). Ultrapure water

type 1 was used in blanks and reagents. Precision varied across compounds, and the wide range of concentrations analyzed: 3–20% relative standard deviations. Accuracy was better than 5% in all analyses. Analytical quality assessment was performed using ion balance, ion-calculated vs. measured conductivity, and ion-estimated vs. measured alkalinity (Moiseenko et al. 2013). Samples with marked deviations corresponded to low ionic strength, which showed overestimated calcium (1) or magnesium (4) levels, which were substituted by zero values in the numerical analyses. Chloride was not considered in the factorial analysis because of the high number of values below the quantification limit. For other variables, limits of quantification were used in the numerical analyses (Table 2). During the 2014–2015 laboratory analysis, no aluminum measures were performed. However, for a subset of 10 lakes of the original survey, aluminum data were available from monthly sampling during 2019–2020, which were only used to confirm some mineral equilibrium assumptions.

Geomorphology, lithology, and land cover

Three main drivers important for water chemistry variation were considered: the parent rock, the ultimate primary source of solutes; land cover, which may condition water–rock interactions; and watershed and waterbody morphology that may determine the interaction duration. Climate is relatively similar across the survey area (Padrón et al. 2015); therefore, altitude was the only variable considered as a surrogate of potential climatic effects.

Lake and watershed geomorphological descriptors (1 : 5000) were available from Mosquera et al. (2017*b*), whose site coding was maintained. Geological information was extracted from a 1:100,000 geological map (Dunkley and Gaibor 2009), which was used to calculate the area of the main lithostratigraphic classes for each lake watershed. The Cajas bedrock corresponds to a complex imbricate layering of volcanic formations (i.e., eight in the surveyed lakes) of varying age (7–37 Ma), from the late Eocene to Miocene, and some minor areas of intrusive rocks (Supporting Information Table S1; Fig. S1). The geological formations vary in dominant parent rock (rhyolite, andesite, dacite, and diorite) and material (tuffs, breccia, lava, lapilli, and sandstone), but all of them show a large secondary variability within the formation.

Although the páramo landscape appears relatively homogeneous at first glance, lake watersheds may markedly differ in vegetation cover and development (Fig. 2). The identified land cover classes included páramo grassland vegetation (e.g., *Calamagrostis*), *Loricaria* and *Gynoxis* shrubs, *Polylepis* open forest, montane evergreen forest, rocky páramo, bare rock, eroded land, wetlands, rivers, and water bodies (Supporting Information Fig. S2). The land covered by the respective classes was uneven (Supporting Information Table S2), and the montane forest was exclusively present in the Lake Llaviucu watershed. The land cover map was

Table 2. Summary of the water chemistry variation in the study lakes of the Cajas Massif, Southern Ecuadorian Andes.

Variable	Units	Minimum	First quartile	Median	Mean	Third quartile	Maximum
Conductivity	μS_{20} cm^{-1}	4.3	28	48	52	69	191
pH		4.6	6.6	7.0	7.0	7.5	8.5
Calcium	μeq L^{-1}	~ 0*	200	400	457	640	1922
Magnesium	μeq L^{-1}	~ 0*	71	116	138	194	697
Sodium	μeq L^{-1}	5	29	44	47	61	117
Potassium	μeq L^{-1}	< 3†	< 3†	3	4	6	37
Alkalinity	μeq L^{-1}	47	260	440	525	720	2208
Sulfate	μeq L^{-1}	10	55	76	88	104	343
Chloride	μeq L^{-1}	< 10†	<10†	< 10†	—	< 10†	30
Silica	μmol L^{-1}	13	67	90	90	108	196
Nitrate	μeq L^{-1}	0.01	0.02	0.15	0.26	0.34	2.8
TP	μmol L^{-1}	0.02	0.12	0.22	0.26	0.31	1.40
SRP	μmol L^{-1}	< 0.02†	< 0.02†	< 0.02†	0.05	0.05	0.61
TOC	mg L^{-1}	0.15	3.6	5.0	5.9	6.6	> 21†
DOC	mg L^{-1}	0.15	2.1	3.0	4.1	5.3	> 21†
Apparent color	CU	7	20	28	37	39	187
Iron	μmol L^{-1}	0.18	0.64	1.07	1.71	1.92	15.25
Manganese	μmol L^{-1}	0.05	0.11	0.25	0.43	0.48	5.04
Aluminum‡	μmol L^{-1}	1.30	1.83	1.97	2.11	2.15	3.20

*Estimated by cation–anion balance because below quantification limits (20 μeq L^{-1} for calcium and magnesium, and 15 μeq L^{-1} for chloride).
†Beyond quantification limit values.
‡Data only for 10 lakes. Ammonium was below the quantification limit (1 μeq L^{-1}) in all lakes.

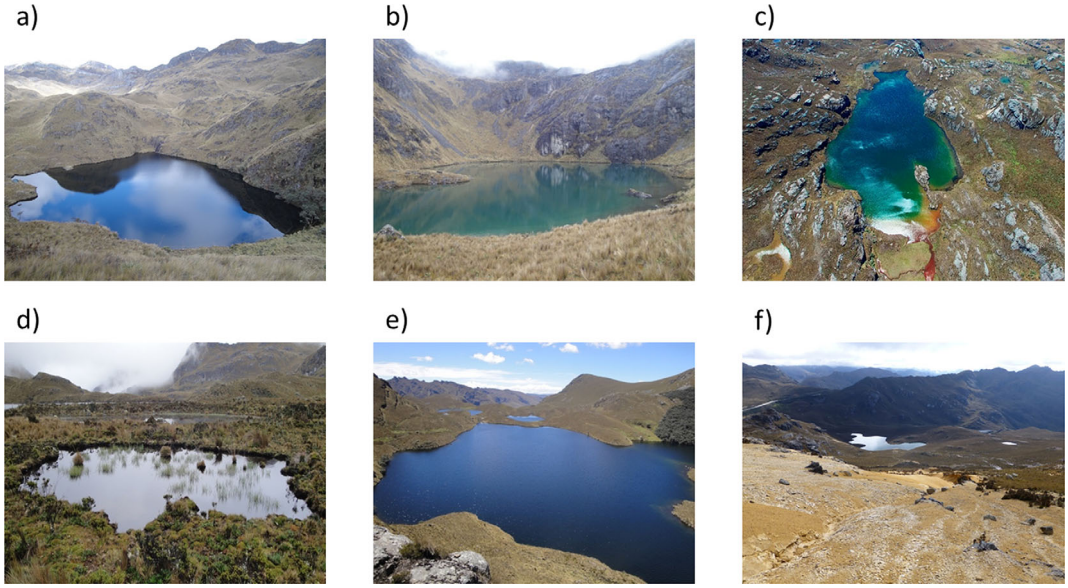

Fig. 2. Some illustrative lakes and landscapes from Cajas Massif in Southern Ecuadorian Andes: (**a**) Laguna de la Cascada, #99; (**b**) Cardenillo, #100; (**c**) Cocha totorilla 1, #149; (**d**) Ingacasa, #36; (**e**) Estrellascocha de Quitahuayco; and (**f**) example of the land cover class "eroded land."

produced by heads-up digitalization of the aerial photographs of the project SIG-Tierras (2010–2014, www.sigtierras.gob.ec). The images (30×30 cm^2 resolution) were orthorectified and georeferenced. Only one digitizer performed the manual task for consistency, and several people repeatedly checked for omissions and mistakes. ArcGIS 10.0 (ESRI Inc.) was used with a screen zoom of the photographs consistently below a 1:200 scale. The scale of cartographic digitalization was 1:5000. The area of each land cover class within the lake watershed was calculated from the digitized land cover contour shapefile, and the lake watershed shapefile (3×3 m^2 resolution) using the ArcGIS 10.0 analysis tools and summarize function.

Numerical analyses

Descriptive statistics, analyses of variance, Tukey's honest significant differences, and other statistical analyses detailed below were performed using R (v. 4.0.4). Except for pH and silica, most water chemistry components had a skewed distribution; hence they were log-transformed in numerical studies. Maximum likelihood factor analysis (*factanal* R-function) was used to investigate the correlation structure among the water chemistry variables. Varimax rotation was applied to facilitate axis interpretation, and the optimal number of factors was determined using the nFactors R-package. The influence of potential drivers on the main water chemistry variation was investigated using multivariate linear regression (*lm* R-function) based on altitude, geomorphological, lithological, and landcover descriptors. Fifteen explanatory variables were considered; lake mean depth, watershed/lake area ratio, main rock proportions (rhyolite, dacite, and diorite), geological formation age, land cover proportions (páramo, rocky páramo, *Polylepis* forest, shrubs, bare rock, eroded land, water bodies, and wetlands), and altitude. Andesite, the most common substrate across lake basins, determines the typical conditions from which other substrates can cause deviations. Therefore, only the percentages of the other 3 substrates were included as potential deviations from the andesite norm. Drivers with skewed distributions were log-transformed (i.e., mean depth, watershed/lake ratio), and all of them were standardized (*z*-scores) to obtain coefficients that directly indicate the degree of influence in the regression. We ranked all possible models (2^{15}) using the corrected Akaike's information criterion (AIC_c), which is more appropriate for relatively small datasets, and the *dredge* function from the MuMIn R package (v.1.43.17). Regression coefficients were standardized to allow comparisons of their relative magnitudes between the models. The coefficients of all models with an $AIC_c < 4$ higher than the lowest AIC_c were averaged (*model.avg* function): the coefficient absolute mean deviation from zero indicates the variable explanatory capacity and the coefficient range shows the uncertainty associated with that deviation (Dormann et al. 2018). Speciation and solubility diagrams were determined using Geochemist's Workbench® (Aqueous Solutions LLC), version GWB 2021, SpecE8, and Act2 programs, respectively (Bethke 2008).

Results

Water chemical variation

The Cajas lakes typically showed low ionic content, circumneutral pH, low nutrient, and slightly brownish conditions (Table 2). Although the ionic content was relatively low (conductivity always < 200 μS_{20} cm^{-1}), most water bodies were

not sensitive to acidification (alkalinity > 200 μeq L^{-1}). Acidic water bodies (i.e., pH < < 6.5) were uncommon and limited to small ponds. Calcium was commonly the dominant cation, although magnesium also showed high values and was dominant in a subset of lakes (Fig. 3). The potassium concentration was extremely low compared to other cations, including sodium. Bicarbonate and sulfate could be dominant among the anions (Fig. 2), yet the latter was not associated with acidic conditions. Chloride levels were generally below quantification limits (Table 2), which indicated an atmospheric origin consistent with the low chloride content (< 10 μeq L^{-1}) in the deposition of Southern Andes (Beiderwieden et al. 2005). High values (~ 30 μeq L^{-1}) were only found in the Quinuas river basin, close to the only mountain road crossing the study area, which connects Cuenca and Guayaquil cities (e.g., lakes 81–83, Fig. 1). Nitrogen components had extremely low concentrations; ammonium was always below the quantification limit, while nitrate concentration seldom exceeded > 1 μeq L^{-1}. Phosphorus values were also usually low; therefore, water bodies were oligotrophic, with few exceptions. The lake color ranged from crystal clear to reddish and brown tones. Accordingly, organic matter (TOC and DOC) and iron content revealed a wide variation (Table 2).

The chemical variables showed clear correlation patterns (Supporting Information Fig. S3). The factor analysis indicated that these relationships could be summarized by four main latent factors, which explained 53% of the total variance (Table 3). *F*1 could be interpreted as a total ionic strength factor, provided mainly by calcium and magnesium cations (water hardness) that primarily determined alkalinity and conductivity values, with a secondary sodium contribution (Table 3). The higher the *F*1 score, the lower the apparent color and TP. Therefore, the higher the alkalinity, the more transparent and less productive the environment becomes. *F*2 denoted the organic matter content, which appeared largely independent of the inorganic chemical characteristics, and was only weakly associated with the apparent color.

*F*3 was primarily related to silica and monovalent cations, indicating a more congruent dissolution of aluminum–silicate minerals than *F*1. The association of sulfate with this factor, although weak, might point to a particular bedrock type. Finally, *F*4 was characterized by metals, particularly iron. Interestingly, the iron present was not strongly bonded to organic content. Indeed, the apparent color showed a higher loading on *F*4 than *F*2, likely related to the reddish color when the iron level was very high. TP (positively) and nitrate (negatively) were associated with *F*4, indicating that water bodies richer in metals tend to be slightly more productive.

Table 3. Variable loadings on four significant main axes (*F*1–*F*4) of a water chemistry factorial analysis.*

Variable	*F*1	*F*2	*F*3	*F*4
Log (alkalinity)	0.98		0.17	
Log (conductivity)	0.91		0.29	
Log (calcium)	0.90			
pH	0.70		0.17	
Log (magnesium)	0.50			
Log (TOC)		0.98		0.16
Log (DOC)		0.77		
Log (sodium)	0.41		0.83	
Silica		−0.20	0.74	
Log (potassium)			0.43	0.34
Log (sulfate)			0.26	
Log (SRP)			−0.22	0.14
Log (iron)	−0.18			0.93
Log (manganese)				0.56
Log (apparent color)	−0.34	0.33	−0.22	0.50
Log (TP)	−0.31			0.23
Log (nitrate)				−0.17

*Only loadings > |0.14| are shown. Factors explained 22%, 11%, 10%, and 10% of the total variation, respectively.

Drivers of water hardness variation

Chemical rock weathering should be connected to both the *F*1 and *F*3 axes of the factor analysis. They should, however,

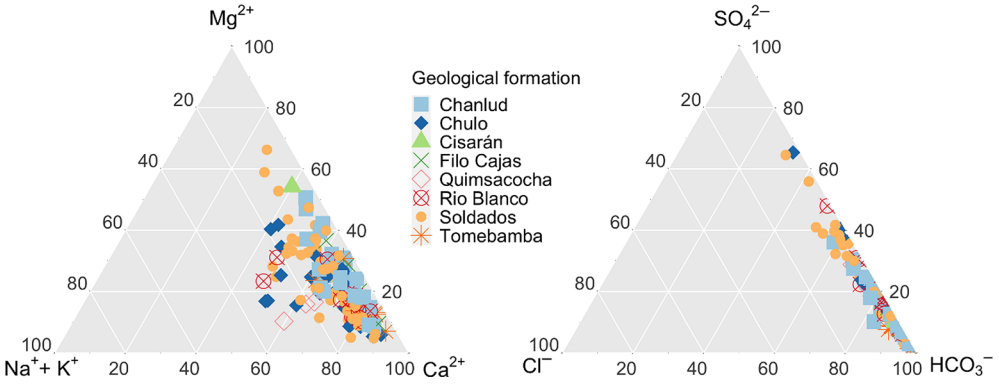

Fig. 3. Ternary diagrams of the relative ionic water composition of the study lakes. Symbols indicate the predominant geological formation in the lake watershed.

be linked to different underlying processes because they emerge in the factor analysis as orthogonal components, indicating independence. Alkalinity and conductivity high loadings on *F*1 link the factor to a dominant rock weathering process. High calcium and magnesium (hardness) contributions to *F*1, but not silica, point to a noncongruent mineral dissolution of aluminum–silicates bearing divalent cations and consequently forming secondary minerals that retain silica. Given the wide alkalinity and conductivity range, this primary process should be highly variable across space (Table 2). Indeed, the geological formations showed significant differences in water hardness (Fig. 4a). The high variability within formations was initially unexpected because the lithological composition in most formations comprised andesite and dacite in varying proportions and mixed volcanic materials (Supporting Information Table S1). Rhyolite, which in principle is less weatherable, only predominated in the Chulo unit, which indeed showed lower than average ionic strength.

Interestingly, the differences in divalent cation levels (and thus ionic strength, alkalinity, and weathering rates) between the geological formations corresponded to their age within the andesite–dacite dominion. The older the volcanic formations, the higher the cation levels (Fig. 4a). Formations of comparable age (i.e., Tomebamba-Filo Cajas, Rio Blanco-Chanlud) showed similar hardness distributions. In contrast, Chulo formation (rhyolite) showed significantly lower hardness levels than the closest andesite-dacite formation by age.

Despite the general rock type and age patterns, *F*1-related variables showed broad variability within some formations (i.e., Soldados, Chanlud, Chulo). Part of this variation could be because some lakes included more than one formation in their watersheds, although this is not a common feature

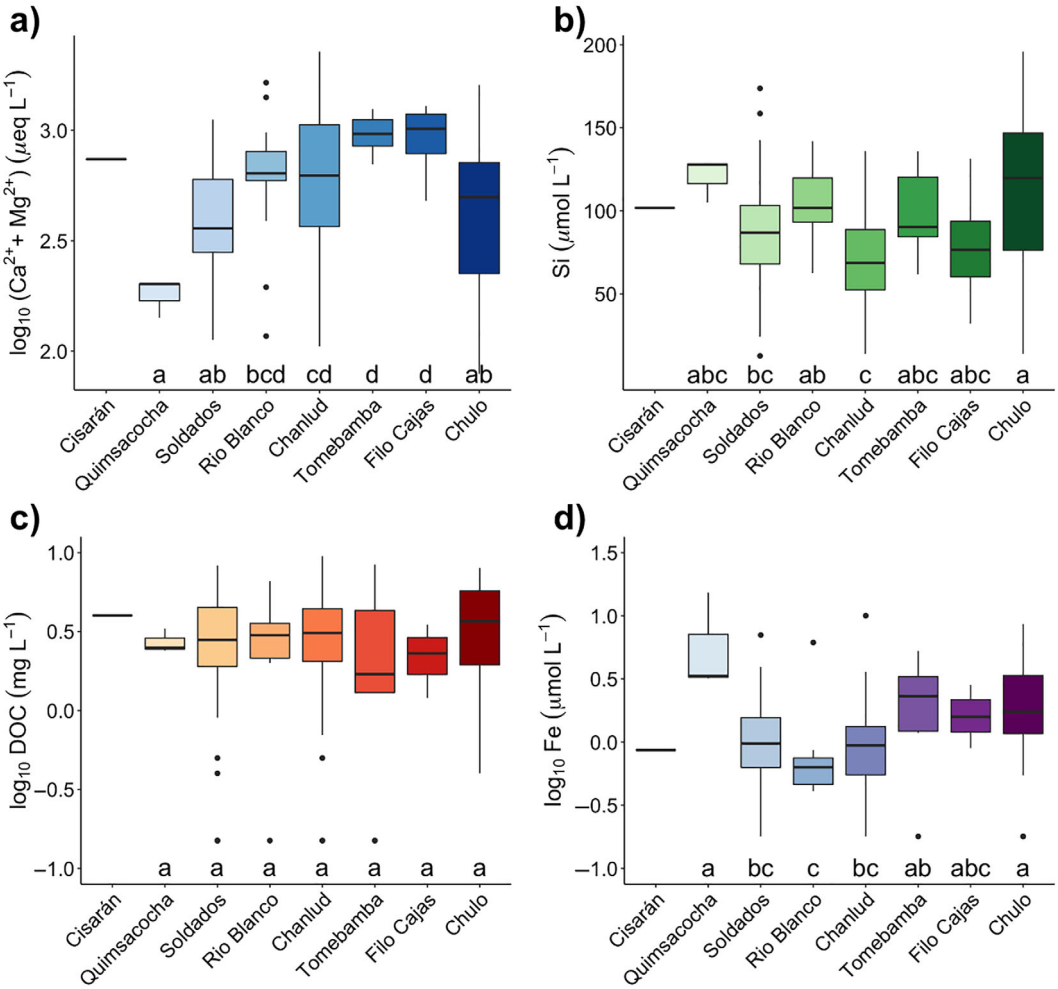

Fig. 4. Chemical variation distribution within the geological formations: (**a**) water hardness (calcium + magnesium), (**b**) silica, (**c**) dissolved organic carbon, and (**d**) iron. The four chemical components were selected to represent the four axes of the factorial analysis (Table 3). Each lake was assigned to the geological formation with the highest percentage in the watershed. Sharing a lower case letter on the *x*-axis indicates a nonsignificant mean difference between a pair of geological formations (*p*-value, >0.05). The number of lakes, characteristics, and geographical distribution of the geological formations are shown in Supporting Information Table S1 and Fig. S1, respectively.

(Supporting Information Table S2). Therefore, most of the variability should be due to other weathering drivers that may increase the contact between water, carbon dioxide, and minerals. The multivariate regression analysis confirmed, with low uncertainty, that water hardness was favored by rock age and limited by rhyolite (Fig. 5a).

The most significant hardness drivers were geomorphological variables (i.e., mean depth and watershed/lake area ratio). Increasing the hardness with watershed and waterbody size indicated an accumulation process in the drainage basin. In contrast, the influence of land cover features was less conclusive in the models; the coefficients showed considerable variability (Fig. 5a). Wetland, bare rock, and *Polylepis* forest showed positive coefficients in the models. They might enhance the divalent cation content by providing more substrate or moisture and CO_2 at the interface where weathering occurs. Páramo and rocky páramo influence were highly uncertain; despite some models showing the highest coefficients, they were inconsistently positive or negative, depending on the combination with other variables. To understand the effect of vegetation in weathering, finer resolution in vegetation, soil, and topography details is required. Overall, these models explained approximately 36% of the total hardness variation.

Drivers of silica variation

The contribution of silica to the *F*3 axis in the factorial analysis and the poor loading of divalent cations suggested a secondary weathering process. There were marked average differences between the geological formations (Fig. 4b). However, the differentiating patterns changed from those shown by hardness, which is a clear indication that the causal drivers for *F*1- and *F*3-related variables were relatively independent. Indeed, the multivariate regression models showed that

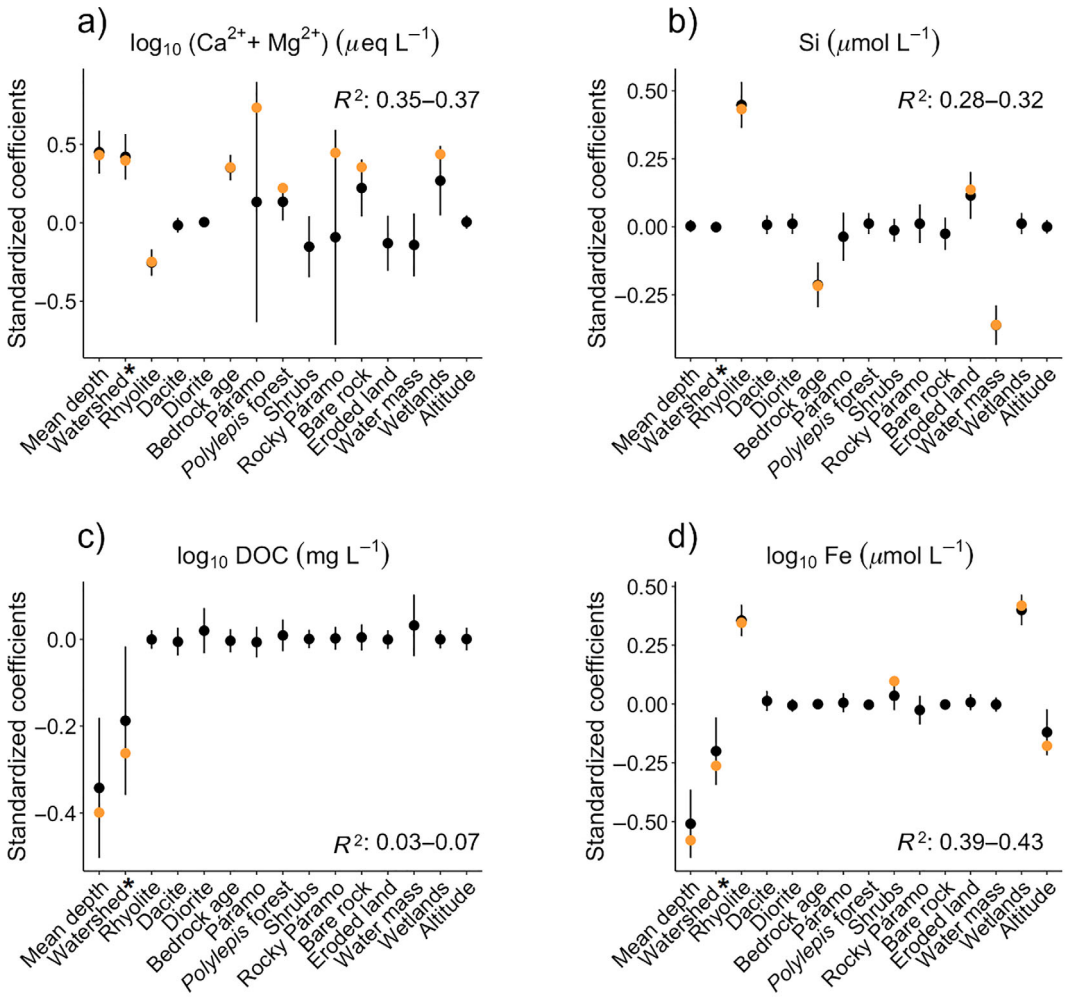

Fig. 5. Driver significance for selected water chemistry components: (**a**) hardness (calcium + magnesium); (**b**) silica; (**c**) dissolved organic carbon; and (**d**) iron. The plots indicate the mean and range of the standardized regression coefficients of multivariate models with a < 4 AIC_c difference from the best model (indicated by an orange dot). All possible models (2^{15}) were assessed and ranked by the lowest AIC_c. The larger the mean departure from zero and the smaller the range of coefficients, the greater the probability of relevance of the driver. The range of variance explained (R^2) by the selected models is included in the plots. (*) Watershed/lake area ratio.

geomorphological features were not significant for silica levels (Fig. 5b), in contrast to the water hardness case.

Despite the high variation in calcium levels, the relatively constrained silica concentration indicated oversaturation or equilibrium of secondary silicates, such as kaolinite ($Al_2Si_2O_5(OH)_4$) clay (Fig. 6a). Only a few cases were more likely related to aluminum hydroxide minerals (i.e., gibbsite, $Al(OH)_3$); those with the lowest silica levels.

Rhyolite bedrock contributed positively to silica levels, while rock age contributed negatively, just opposite effects of drivers than on hardness. The presence of eroded land in the watershed had a positive effect. This landscape feature occupies only a small part of the overall territory (Fig. 2e); it may have a marked influence when it is present. The proportion of water mass in the watershed resulted in a pronounced negative effect on silica levels, likely related to biological consumption (e.g., diatoms).

Overall, the regression models explained approximately 30% of silica variation. The patterns found, particularly the decline with rock age and association with eroded land, suggested some relationship with secondary volcanism processes with less extension and more random spatial distribution, which may be exhausted over time. The lack of any relationship with watershed or lake geomorphological features indicates that source areas are relatively small and do not show accumulative effects at the watershed scale.

Drivers of organic matter variation

The organic matter content in lake water (*F2* in the factor analysis) did not differ between geological formations (Fig. 4c). Indeed, the regression models only showed some relevance of the geomorphological variables (Fig. 5c). The smaller the lake and its watershed, the higher the DOC levels that could be expected. Although these parameters were significant, their explanation was limited (~ 5% of the overall variation), indicating high DOC scattering regardless of lake depth (Supporting Information Fig. S4) or watershed size.

Drivers of metal variation

There were significant differences in the metal levels among the geological formations (Fig. 4d). The concentrations were higher on average in Chulo, Filo Cajas, Tomebamba, and, particularly, Quimsacocha, although only three lakes were sampled in the latter case. The variation was substantial in the other formations, and the higher values overlapped with those in the metal-rich formations.

High iron levels were more likely in small water bodies with smaller watersheds (Fig. 5d), as occurs for DOC, indicating that point sources were not evenly distributed in the landscape. These point sources were markedly more when the rhyolite bedrock was dominant. In addition, the higher the proportion of wetlands in the watershed, the higher the iron levels. These significant drivers accounted for approximately 41% of the variation. Altitude (negatively) and shrubs (positively) contributed appreciably to some models, but the general uncertainty may indicate a spurious contribution.

Water bodies with higher iron concentrations were oversaturated (Fig. 6b). In some lakes, iron precipitation was particularly evident and colorful, associated with inlets connected to wetlands (Fig. 2f). As the metal levels declined and the pH

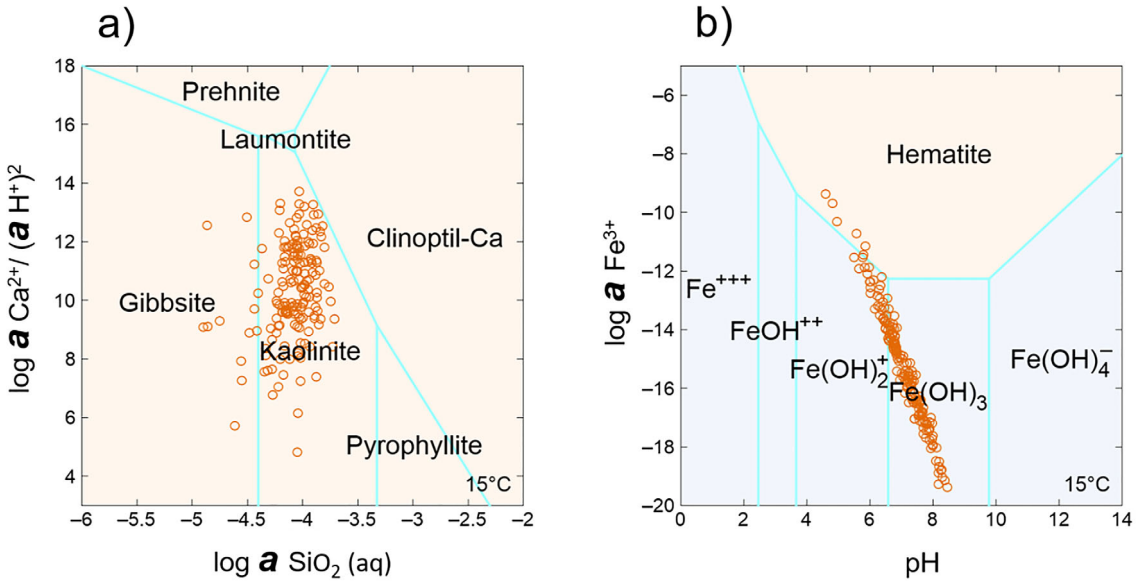

Fig. 6. Water chemistry position of the lakes in theoretical stability diagrams. (**a**) Mineral stability in a system with varied activities of calcium and silica, and activity = 1 of aluminum (in mineral form) and water. (**b**) Iron solubility assuming a 0.0002512 oxygen fugacity; an average oxygen value in the surface lake water samples. Temperature was fixed at 15°C in both cases. Reddish background indicates a solid phase, while bluish background represents an aqueous form. Calculations were performed using GWB 2021.

increased, soluble iron hydroxide forms were more likely to occur. Nevertheless, some measured iron could be associated with colloidal and small particles in lakes where hematite (Fe_2O_3) oversaturation is indicated.

Discussion

Water chemical variation and rock weathering

Our results show that high mountain lakes in volcanic basins can present extremely variable water chemistry in relatively small areas. The variation found in Cajas NP was comparable to that in large mountain ranges (Fig. 7; Supporting Information Fig. S5 for pH), where the substrate includes plutonic, metamorphic, and carbonate bedrock changing over large areas (Camarero et al. 2009). Active volcanism produces lava flows that overlap unevenly and heterogeneously distributed tuff, lapilli, and ash. Even more locally, hydrothermal processes reaching the surface create patches of substrate that differ from the dominant rock. Cajas Massif lakes show that this heterogeneity still influences water composition variation in volcanic bedrock dating millions of years. Indeed, the spatial heterogeneity and eventual water chemical variation may be increased by the presence in the watersheds of layers corresponding to several volcanic phases that differ in dominant rock, age, and associated secondary processes.

Lakes on watersheds where rhyolite bedrock dominated had softer water than lake basins where andesite, dacite, or diorite predominated. The latter rock types are richer in plagioclase and pyroxene, which are minerals that are more easily weathered than quartz and orthoclase (White and Brantley 1995). Calcium and silica levels indicate that the weathering of these primary minerals is not complete; secondary silicates, most likely kaolinite, are formed. This incongruent dissolution has been found in other volcanic rock areas (Di Figlia et al. 2007). The high correlation of calcium with alkalinity and conductivity indicates that this partial aluminosilicate dissolution is the primary source of cations. Recent studies of Cajas' andesitic soils indicate that they are depleted in mono- and divalent cations with an accumulation of Al-humus complexes in the soil matrix (Molina et al. 2019) even though these soils are postglacial and therefore relatively young. Consequently, water alkalinity generation primarily occurs in the subsoil saprolite, which explains why water hardness increases with watershed and lake size. The cation excess increases the longer the water travels through the subsurface before reaching the lake or pond.

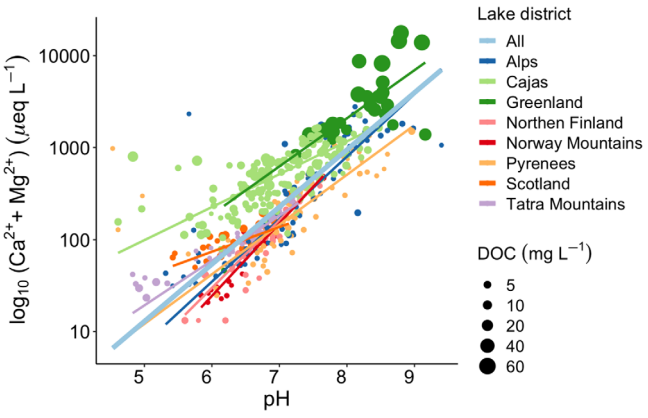

Fig. 7. Relationship between pH and divalent cations in several lake districts in temperate mountain ranges and boreal areas (data from Catalan et al. 2009*b*) for comparison with Cajas NP (this study data). Theil-Sen linear robust regression (*mblm* R package) was applied to downscale the influence of the outliers, mostly from waters affected by sulfide oxidation. High DOC waters show a higher intercept due to the effect of organic acids on pH.

In addition to rock type, the surface area available for the reaction influences weathering rates (White and Brantley 2003). Older volcanic bedrock presents higher porosity and surface area for hydration and reaction. Our results indicate that the age of the geological formation is a significant driver for divalent cation levels and alkalinity. This finding is consistent with 5-yr field investigations that indicate that older rhyolite rocks with similar initial compositions have faster chemical weathering rates than younger ones (Matsukura et al. 2001). The significance of the bare rock proportion in the watershed also points to the same mechanism, as these outcrops are usually heavily fractured, providing more and fresher surfaces for reaction (Kopáček et al. 2017). Vegetation has been identified as a factor promoting weathering (Burghelea et al. 2015) because it increases the availability of carbon dioxide and protons; however, our results were inconclusive. Páramo and rocky páramo both show positive and negative effects depending on the regression model. Conversely, the role of wetlands appeared robust; it always indicated weathering enhancement when included in the regression models. Nevertheless, there is still a considerable proportion of the hardness variation to be explained. Molina et al. (2019) showed a significant difference in soil chemical weathering related to topographic gradients and vegetation change at spatial scales that cannot be documented in our macroscale landscape study. The uncertainty associated with vegetation variables in the multiple regressions could be related to the lack of resolution at fine spatial scales.

Our factorial analysis suggested a complementary weathering process beyond the predominant cation source. Silica levels, which indicate complete aluminosilicate dissolution, were associated with monovalent cations and sulfate as part of a third main orthogonal factor. The silica drivers identified in the multivariate regression analysis supported the interpretation of an independent complementary weathering process. It was not related to the size of the watershed or the lake; hence, it did not have an extended occurrence that could sustain an accumulative process like that of divalent cations. This process likely occurs in hot spots sparsely distributed in watersheds. The association with eroded land was also noted in this local character. Furthermore, contrary to the hardness

factors, silica levels were favored in the rhyolite bedrock and declined with rock age. This evidence points to a bedrock affected by former hydrothermal processes, which occur during periods of active volcanism (Pozzo et al. 2002). High water temperatures modify the original aluminosilicates, making secondary ones deficient in cations (Ohba and Kitade 2005) and other processes such as albitization (Engvik et al. 2008). The latter may eventually result in chemical weathering, providing sodium (Cruz et al. 1999). The hydrothermal activity may or may not be associated with sulfur. Both types have been described in the Quimsacocha formation during exhaustive mining prospecting (Morán-Reascos 2017). There is no reason to think that they are not present in other formations, particularly in the Chulo unit, where rhyolite predominates, and thus the likely contingent association with this bedrock in the driver analysis. The decline with the formation age indicates that this original mineral material was not replaced by rock fragmentation, which makes sense if these are spots in the landscape where the initial rock already consists of secondary aluminosilicates, which offer more reaction surfaces (e.g., clays), and thus can provide locally higher silicate values. Sodium-rich volcanic rocks can also be related to tectonic processes (Sun et al. 2020), and faults could be another location for this particular weathering.

Weathering occurring in two distinct environments has been described in other tropical watersheds (White et al. 1998). Plagioclase and hornblende reacted at the heavily fractured bedrock—the saprock interface, as likely occurred in our case. Secondarily, biotite and quartz reacted preferentially in the overlying thick saprolitic regolith, providing more K, Mg, and Si to water chemistry. This latter mechanism shows Si delivery in common with our case but differs in the main cations (i.e., Mg). Overall, independent weathering mechanisms seem to be more likely in tropical volcanic watersheds than in temperate watersheds with less intense weathering. Investigating the water systems (streams, subsurface, ponds, and lakes) associated with the eroded land identified in the land cover classification and areas with tectonic faults should shed light on our conjectures.

Silica levels were negatively affected by the water mass proportion in the watershed. This relationship points to aquatic biological consumption without evidence of terrestrial biological pumping effects, as found in other volcanic areas (Benedetti et al. 2002). In contrast, the observed low potassium levels could reflect uptake by terrestrial plants.

No specific atmospheric chemical deposition studies have been conducted in the Cajas NP area. Occasionally, dust deposition arriving at the equatorial Andes as far as the Sahara desert may provide divalent cations (Boy and Wilcke 2008), and biomass burning in the Amazon basin may provide acidifying sulfur and nitrogen compounds, as found in other areas of Southern Ecuador (Fabian et al. 2005). However, it is not possible to evaluate the deposition incidence on the average chemical composition of lakes and its variation without specific studies. ANC in the Cajas waterbodies is usually high (> 200 μeq L^{-1}), but some sensitive sites could be influenced by atmospheric deposition. Low chloride levels indicate that most of the deposition is from westward air masses. However, significant rainfall episodes from the Pacific have been described for nearby areas during the wet season, bringing high salt deposition (Makowski Giannoni et al. 2016). Therefore, atmospheric deposition can provide seasonal and interannual variability in Cajas Massif waterbodies. Higher chloride values associated with the only road across the park indicate the system sensitivity.

Brown waters

Average and extreme DOC levels are higher in Cajas Massif lakes than in temperate mountain lake districts (Fig. 7) and similar to some boreal areas (Camarero et al. 2009). In contrast to cations related to rock weathering, DOC is higher in ponds and small lakes with relatively small watersheds. These features indicate a relatively local DOC origin, likely related to the idiosyncratic connections with organic soils proximal to the water body. Land cover features that apparently should be relevant for DOC (Gergel et al. 1999), such as the wetland percentage in the watershed, did not significantly influence our case.

In boreal watersheds, stream DOC originates predominantly from wetland sources during low flow conditions and from forested areas during high flow (Laudon et al. 2011), and detailed hydrology is becoming an essential component of DOC regulation. In the Cajas Massif, extreme values were achieved in small ponds, which are sometimes marginal to other water bodies. As these systems are very shallow, they are not fed with subsoil water but by water draining from immediate surface soils lacking buffering capacity. Consequently, these ponds had lower pH values (~ 5). Comparing across lake districts with significantly different average DOC levels (Fig. 7), Cajas' lakes align with high DOC lake districts (e.g., Greenland) in the relationship between divalent cation levels (or alkalinity) and pH. In these high DOC lake districts, the average pH was lower at the same alkalinity than in low DOC lake districts, showing the relevance of organic acids in providing acidity. Although the direct correlation between pH and DOC is low in Cajas waters, DOC becomes a significant parameter explaining residuals between pH and hardness; therefore, a better fit was obtained with multiple regression ($pH = 6.37 + 0.0012$ hardness $- 0.026$ DOC; $R^2 = 0.46$).

Nevertheless, paludification is not a generalized feature in Cajas lakes and ponds, and a wide range from clear to brownish water was found. Indeed, the apparent color is related to organic matter and metal content, yet there is no strong correlation between the latter two, indicating different sources. The chelation of metals may occur in high DOC systems, but there are lakes with high iron content and low DOC in the Cajas Massif. The organic and metal contents in the Cajas lakes do not share the same main drivers. Compared to iron levels, the drivers' low DOC explanatory capability necessitates an ad

hoc investigation of DOC composition and sources in the páramo lakes.

High iron availability

Iron levels are generally high; however, similar to DOC, the smaller the water body and its watershed, the higher the probability of finding elevated values. The differences between the several geological formations were significant and reflect the idiosyncrasies of the volcanism in each, with rhyolite bedrock resulting in increased iron levels. Nevertheless, the driver with more influence was the proportion of wetlands in the watershed. Water in wetlands may achieve lower pH and redox potential, thus facilitating iron solubility. Lake surface layers are usually well-oxygenated and foster iron precipitation, evident in some colorful lake littoral beds (Fig. 2f). Some iron may remain in colloidal form, as measured concentrations often indicate oversaturation.

Interestingly, TP was associated with iron and manganese in the factorial analyses. Therefore, some iron sources may also provide essential nutrients for primary production. Apatite-bearing iron deposits can be associated with magmatic-hydrothermal events (Allen et al. 1996). Our study considered only lake surface samples. Although dominant cations may change little throughout the water column, this is not the case for metals, whose solubility depends on redox conditions. Because of the persistent stratification, many of these lakes show oxygen depletion in deep layers (Steinitz-Kannan et al. 1983). These layers provide an environment for reduced metal forms and other reduced compounds, such as ammonium, which are undetected in surface waters. The anoxic conditions also facilitate phosphate solubility; therefore, the correlation between iron and phosphorus is possible because of watershed sources or in-lake processes.

Ecological implications

Main ion composition and dissolved organic matter are two primary factors influencing the biota distribution in high-mountain lakes (Kernan et al. 2009). The chemical variation found in Cajas Massif lakes and ponds is comparable to that of all the European mountain ranges (Fig. 7). Therefore, a small area and relatively homogeneous bedrock provide a variety of aquatic chemical niches that is equivalent to large territories of contrasting bedrock. This remarkable feature might foster species richness in relatively small territories of aquatic organisms that are sensitive to cation composition. The Cajas alkalinity range includes the two ecological thresholds (i.e., ~ 200 and ~ 1000 μeq L^{-1}) identified in European mountain ranges in terms of community composition (Catalan et al. 2009*a*). Diatoms and some crustaceans show this nonlinear community response to the alkalinity gradient, which will be interesting to confirm in this far-flung lake district, which shares with European ranges many diatom species (Benito et al. 2019), but not crustaceans (Catalan and Donato-Rondón 2016).

In these volcanic environments, a biologically interesting factor is the Ca : Mg ratio variation (Fig. 3), which is probably related to variations in andesite plagioclase and hornblende proportions. The biological influence of the dominant divalent cation type has been barely explored as a driver of species segregation in aquatic mountain ecosystems, probably because of the lack of a balanced number of sites. Organisms with carbonate shells (e.g., ostracods, mollusks, etc.) are candidates to respond to this factor, as found in other aquatic ecosystems (Dussart 1976; Chivas et al. 1986).

Soils largely depleted in cations enhance the chemical contrast between lakes and ponds. Small and shallow ponds may lack the inflow of water circulating below the soils; consequently, some show the most acidic water or high DOC content, favoring biotic differentiation (Catalan et al. 2009*a*). We considered many ponds in our study, but many smaller ones exist in the area (Mosquera et al. 2017*a*); thus, more extreme pH and DOC conditions can be expected in some of them. DOC and TOC levels in the Cajas massif are higher than in temperate high-mountain lakes and comparable to Nordic mountain lakes and tundra lakes (Camarero et al. 2009). However, these high-latitude lakes freeze during winters, a feature non-present in the páramo that may have driven adaptation in other directions. In this regard, tropical high-mountain lakes are unique. Apart from the high average level, DOC has a wide range, making it a possible axis of nonlinear species segregation that might include a wide range of organisms (e.g., rotifers, crustaceans, and chironomids), as has been observed in temperate high-mountain lakes with narrower DOC ranges (Catalan et al. 2009*a*).

Metals provide a further environmental gradient for biodiversity enhancement, which is not necessarily linked to the organic matter content of water. Vertical redox gradients have been observed in these tropical lakes (Steinitz-Kannan et al. 1983), but specific investigations concerning species adaptations are lacking. Furthermore, horizontal redox gradients from lakes to neighboring wetlands also likely foster species segregation.

The high chemical variability in tropical high-mountain lakes makes them ideal as global change sentinel lakes; some are more susceptible to acidic or dust deposition, while others are better suited to temperature changes impacting redox conditions. In addition, the long, independent chemical gradients offer the possibility of developing local calibration sets for paleoenvironmental reconstructions using indicator organisms, particularly diatoms (Rivera-Rondón and Catalan 2020). Given the high lake heterogeneity, surveillance and reconstructions may require a thoughtful selection of lakes for making meaningful inferences.

Data availability statement

The data supporting this study are available in Zenodo at https://doi.org/10.5281/zenodo.6506282.

References

Allen, R. L., I. Lundstrom, M. Ripa, A. Simeonov, and H. Christofferson. 1996. Facies analysis of a 1.9 Ga, continental margin, back-arc, Felsic Caldera province with diverse Zn-Pb-Ag-(Cu-Au) sulfide and Fe oxide deposits, Bergslagen region, Sweden. Econ. Geol. **91**: 979–1008. doi:10.2113/gsecongeo.91.6.979

APHA-AWWA-WEF. 2012. Standard methods for examination of water and wastewater, 22nd ed. American Public Health Association. doi:10.1100/2012/462467

Armienta, M. A., and others. 2008. Water chemistry of lakes related to active and inactive Mexican volcanoes. J. Volcanol. Geotherm. Res. **178**: 249–258. doi:10.1016/j.jvolgeores.2008.06.019

Beamish, R. J., and H. H. Harvey. 1972. Acidification of La Cloche mountain lakes, Ontario, and resulting fish mortalities. J. Fish. Res. Board Can. **29**: 1131–1143. doi:10.1139/f72-169

Beiderwieden, E., T. Wrzesinsky, and O. Klemm. 2005. Chemical characterization of fog and rain water collected at the eastern Andes cordillera. Hydrol. Earth Syst. Sci. **9**: 185–191. doi:10.5194/hess-9-185-2005

Benedetti, M., and others. 2002. Chemical weathering of basaltic lava flows undergoing extreme climatic conditions: The water geochemistry record. Chem. Geol. **201**: 1–17. doi:10.1016/S0009-2541(03)00231-6

Benito, X., and others. 2019. Identifying temporal and spatial patterns of diatom community change in the tropical Andes over the last c. 150 years. J. Biogeogr. **46**: 1889–1900. doi:10.1111/jbi.13561

Bethke, C. M. 2008. Geochemical and biogeochemical modeling, 2nd ed. Cambridge Univ. Press.

Boy, J., and W. Wilcke. 2008. Tropical Andean forest derives calcium and magnesium from Saharan dust. Global Biogeochem. Cycl. **22**: GB1027. doi:10.1029/2007GB002960

Burghelea, C., D. G. Zaharescu, K. Dontsova, R. Maier, T. Huxman, and J. Chorover. 2015. Mineral nutrient mobilization by plants from rock: influence of rock type and arbuscular mycorrhiza. Biogeochem. **124**: 187–203.

Camarero, L., and others. 2009. Regionalisation of chemical variability in European mountain lakes. Freshw. Biol. **54**: 2452–2469. doi:10.1111/j.1365-2427.2009.02296.x

Carrillo-Rojas, G., B. Silva, M. Córdova, R. Célleri, and J. Bendix. 2016. Dynamic mapping of evapotranspiration using an energy balance-based model over an Andean páramo catchment of Southern Ecuador. Remote Sens. (Basel) **8**: 160. doi:10.3390/rs8020160

Catalan, J., E. Ballesteros, E. Gacia, A. Palau, and L. Camarero. 1993. Chemical composition of disturbed and undisturbed high-mountain lakes in the Pyrenees—A reference for acidified sites. Water Res. **27**: 133–141. doi:10.1016/0043-1354(93)90203-T

Catalan, J., and others. 2009a. Ecological thresholds in European alpine lakes. Freshw. Biol. **54**: 2494–2517. doi:10.1111/j.1365-2427.2009.02286.x

Catalan, J., C. J. Curtis, and M. Kernan. 2009b. Remote European mountain lake ecosystems: Regionalisation and ecological status. Freshw. Biol. **54**: 2419–2432. doi:10.1111/j.1365-2427.2009.02326.x

Catalan, J., and J. C. Donato-Rondón. 2016. Perspectives for an integrated understanding of tropical and temperate high-mountain lakes. J. Limnol. **75**: 215–234. doi:10.4081/jlimnol.2016.1372

Cruz, J. V., R. M. Coutinho, M. R. Carvalho, N. Oskarsson, and S. R. Gislason. 1999. Chemistry of waters from Furnas volcano, Sao Miguel, Azores: Fluxes of volcanic carbon dioxide and leached material. J. Volcanol. Geotherm. Res. **92**: 151–167. doi:10.1016/S0377-0273(99)00073-6

Chivas, A. R., P. de Deckker, and J. M. G. Shelley. 1986. Magnesium content of non-marine ostracod shells: A new palaeosalinometer and palaeothermometer. Palaeogeogr. Palaeoclimatol. Palaeoecol. **54**: 43–61. doi:10.1016/0031-0182(86)90117-3

Di Figlia, M. G., A. Bellanca, R. Neri, and A. Stefansson. 2007. Chemical weathering of volcanic rocks at the Island of Pantelleria, Italy: Information from soil profile and soil solution investigations. Chem. Geol. **246**: 1–18. doi:10.1016/j.chemgeo.2007.07.025

Dormann, C. F., and others. 2018. Model averaging in ecology: A review of Bayesian, information-theoretic, and tactical approaches for predictive inference. Ecol. Monogr. **88**: 485–504. doi:10.1002/ecm.1309

Dunkley, P., and A. Gaibor. 2009. Mapa geológico Cordillera Occidental 2°–3°. Hoja geológica Cuenca-NVF 53. Instituto de Investigación Geológico y Energético—Ecuador, Servicio Geológico Nacional, Ministerio de Minas y Petróleos.

Dupre, B., and others. 2003. Rivers, chemical weathering and Earth's climate. C. R. Geosci. **335**: 1141–1160. doi:10.1016/j.crte.2003.09.015

Dussart, G. 1976. The ecology of freshwater molluscs in North West England in relation to water chemistry. J. Moll. Stud. **42**: 181–198.

Eggermont, H., J. M. Russell, G. Schettler, K. Van Damme, I. Bessems, and D. Verschuren. 2007. Physical and chemical limnology of alpine lakes and pools in the Rwenzori Mountains (Uganda-DR Congo). Hydrobiologia **592**: 151–173. doi:10.1007/s10750-007-0741-3

Engvik, A. K., A. Putnis, J. D. Fitz Gerald, and H. K. Austrheim. 2008. Albitization of granitic rocks: The mechanism of replacement of oligoclase by albite. Can. Mineral. **46**: 1401–1415. doi:10.3749/canmin.46.6.1401

Fabian, P., M. Kohlpaintner, and R. Rollenbeck. 2005. Biomass burning in the Amazon-fertilizer for the mountaineous rain forest in Ecuador. Environ. Sci. Pollut. R **12**: 290–296. doi:10.1065/espr2005.07.272

Gergel, S. E., M. G. Turner, and T. K. Kratz. 1999. Dissolved organic carbon as an indicator of the scale of watershed influence on lakes and rivers. Ecol. Appl. **9**: 1377–1390 doi: 10.1890/1051-0761(1999)009[1377:DOCAAI]2.0.CO;2.

Jacobsen, D., and O. Dangles. 2017. Ecology of high altitude waters. Oxford Univ. Press.

Kamenik, C., R. Schmidt, G. Kum, and R. Psenner. 2001. The influence of catchment characteristics on the water chemistry of mountain lakes. Arct. Antarct. Alp. Res. **33**: 404–409. doi:10.2307/1552549

Kernan, M., and others. 2009. Regionalisation of remote European mountain lake ecosystems according to their biota: Environmental versus geographical patterns. Freshw. Biol. **54**: 2470–2493. doi:10.1111/j.1365-2427.2009.02284.x

Kopáček, J., J. Hejzlar, E. Stuchlik, J. Fott, and J. Vesely. 1998. Reversibility of acidification of mountain lakes after reduction in nitrogen and sulphur emissions in Central Europe. Limnol. Oceanogr. **43**: 357–361. doi:10.4319/lo.1998.43.2.0357

Kopáček, J., and others. 2017. Climate change increasing calcium and magnesium leaching from granitic alpine catchments. Environ. Sci. Technol. **51**: 159–166. doi:10.1021/acs.est.6b03575

Laudon, H., and others. 2011. Patterns and dynamics of dissolved organic carbon (DOC) in boreal streams: The role of processes, connectivity, and scaling. Ecosystems **14**: 880–893. doi:10.1007/s10021-011-9452-8

Makowski Giannoni, S., K. Trachte, R. Rollenbeck, L. Lehnert, J. Fuchs, and J. Bendix. 2016. Atmospheric salt deposition in a tropical mountain rainforest at the eastern Andean slopes of south Ecuador–Pacific or Atlantic origin? Atmos. Chem. Phys. **16**: 10241–10261. doi:10.5194/acp-16-10241-2016

Marchetto, A., and others. 1995. Factors affecting water chemistry of Alpine lakes. Aquat. Sci. **57**: 81–89. doi:10.1007/BF00878028

Massabuau, J. C., B. Fritz, and B. Burtin. 1987. Acidification of fresh-waters (pH-less-than-or-equal-to-5) in the Vosges mountains (Eastern France). C.R. Acad. Sci. Paris Life Sci. **305**: 121–124.

Matsukura, Y., T. Hirose, and C. T. Oguchi. 2001. Rates of chemical weathering of porous rhyolites: 5-year measurements using the weight-loss method. Catena **43**: 341–347. doi:10.1016/S0341-8162(00)00129-6

Michelutti, N., A. P. Wolfe, C. A. Cooke, W. O. Hobbs, M. Vuille, and J. P. Smol. 2015. Climate change forces new ecological states in tropical Andean lakes. PLos One **10**: e0115338. doi:10.1371/journal.pone.0115338

Moiseenko, T., N. Gashkina, M. Dinu, T. Kremleva, and V. Khoroshavin. 2013. Aquatic geochemistry of small lakes: Effects of environment changes. Geochem. Int. **51**: 1031–1148. doi:10.1134/S0016702913130028

Molina, A., V. Vanacker, M. D. Corre, and E. Veldkamp. 2019. Patterns in soil chemical weathering related to topographic gradients and vegetation structure in a high Andean tropical ecosystem. Case Rep. Med. **124**: 666–685. doi:10.1029/2018JF004856

Morán-Reascos, D. 2017. Analysis of mineralization extension continuity around the Loma Larga high-sulphidation system. Master Thesis. Univ. Central de Ecuador.

Moser, K. A., and others. 2019. Mountain lakes: Eyes on global environmental change. Glob Planet Change **178**: 77–95. doi:10.1016/j.gloplacha.2019.04.001

Mosquera, P. V., H. Hampel, R. F. Vázquez, M. Alonso, and J. Catalan. 2017a. Abundance and morphometry changes across the high-mountain lake-size gradient in the tropical Andes of Southern Ecuador. Water Resour. Res. **53**: 7269–7280. doi:10.1002/2017WR020902

Mosquera, P. V., H. Hampel, R. F. Vázquez, M. Alonso, and J. Catalan. 2017b. Abundance and morphometry changes across the high mountain lake-size gradient in the tropical Andes of Southern Ecuador. Dryad Dataset. doi:10.5061/dryad.sn058

Murphy, J., and J. P. Riley. 1962. A modified single solution method for the determination of phosphate in natural waters. Anal. Chim. Acta **27**: 31–36. doi:10.1016/S0003-2670(00)88444-5

Nauwerck, A. 1994. A survey on water chemistry and plankton in high-mountain lakes in Northern Swedish Lapland. Hydrobiologia **274**: 91–100. doi:10.1007/BF00014631

Ohba, T., and Y. Kitade. 2005. Subvolcanic hydrothermal systems: Implications from hydrothermal minerals in hydrovolcanic ash. J. Volcanol. Geotherm. Res. **145**: 249–262. doi:10.1016/j.jvolgeores.2005.02.002

Oñate-Valdivieso, F., and others. 2018. Temporal and spatial analysis of precipitation patterns in an Andean region of southern Ecuador using LAWR weather radar. Meteorol. Atmos. Phys. **130**: 473–484. doi:10.1007/s00703-017-0535-8

Padrón, R. S., B. P. Wilcox, P. Crespo, and R. Célleri. 2015. Rainfall in the Andean páramo: New insights from high-resolution monitoring in Southern Ecuador. J. Hydrometeorol. **16**: 985–996. doi:10.1175/JHM-D-14-0135.1

Pozzo, A., and others. 2002. Influence of volcanic activity on spring water chemistry at Popocatepetl Volcano, Mexico. Chem. Geol. **190**: 207–229. doi:10.1016/S0009-2541(02)00117-1

Psenner, R. 1989. Chemistry of high mountain lakes in siliceous catchments of the Central Eastern Alps. Aquat. Sci. **51**: 1015–1621.

Psenner, R., and J. Catalan. 1994. Chemical composition of lakes in crystalline basins: A combination of atmospheric deposition, geologic background, biological activity and human action, p. 255–314. *In* R. Margalef [ed.], Limnology now: A paradigm of planetary problems. Elsevier Science B.V.

Rivera-Rondón, C. A., and J. Catalan. 2020. Diatoms as indicators of the multivariate environment of mountain lakes. Sci. Total Environ. **703**: 135517. doi:10.1016/j.scitotenv.2019.135517

Rogora, M., A. Marchetto, and R. Mosello. 2001. Trends in the chemistry of atmospheric deposition and surface waters in the Lake Maggiore catchment. Hydrol. Earth Syst. Sci. **5**: 379–390. doi:10.5194/hess-5-379-2001

Rollenbeck, R., J. Bendix, and P. Fabian. 2011. Spatial and temporal dynamics of atmospheric water inputs in tropical mountain forests of South Ecuador. Hydrol. Process. **25**: 344–352. doi:10.1002/hyp.7799

Schneider, T., H. Hampel, P. V. Mosquera, W. Tylmann, and M. Grosjean. 2018. Paleo-ENSO revisited: Ecuadorian Lake Pallcacocha does not reveal a conclusive El Niño signal. Glob Planet Change **168**: 54–66. doi:10.1016/j.gloplacha.2018.06.004

Segura, H., and others. 2019. New insights into the rainfall variability in the tropical Andes on seasonal and interannual time scales. Clim. Dyn. **53**: 405–426. doi:10.1007/s00382-018-4590-8

Steffen, W., W. Broadgate, L. Deutsch, O. Gaffney, and C. Ludwig. 2015. The trajectory of the Anthropocene: The great acceleration. Anthr Rev **2**: 81–98. doi:10.1177/2053019614564785

Steinitz-Kannan, M., P. A. Colinvaux, and R. Kannan. 1983. Limnological studies in Ecuador 1. A survey of chemical and physical properties of Ecuadorian lakes. Arch. Hydrobiol. Suppl. **65**: 61–105.

Steinitz-Kannan, M., C. Lopez, D. Jacobsen, and M. D. Guerra. 2020. History of limnology in Ecuador: A foundation for a growing field in the country. Hydrobiologia **847**: 4191–4206. doi:10.1007/s10750-020-04291-1

Sun, Z., and others. 2020. Sodium-rich volcanic rocks and their relationships with iron deposits in the Aqishan–Yamansu belt of Eastern Tianshan, NW China. Geosci. Front. **11**: 697–713. doi:10.1016/j.gsf.2019.06.011

Van Colen, W. R., and others. 2017. Limnology and trophic status of glacial lakes in the tropical Andes (Cajas National Park, Ecuador). Freshw. Biol. **62**: 458–473. doi:10.1111/fwb.12878

White, A. F., and others. 1998. Chemical weathering in a tropical watershed, Luquillo mountains, Puerto Rico: I. Long-term versus short-term weathering fluxes. Geochim. Cosmochim. Acta **62**: 209–226. doi:10.1016/S0016-7037(97)00335-9

White, A. F., and S. L. Brantley. 1995. Chemical weathering rates of silicate minerals: An overview, p. 1–22. *In* A. F. White and S. L. Brantley [eds.], Chemical weathering rates of silicate minerals. Reviews in mineralogy. De Gruyter.

White, A. F., and S. L. Brantley. 2003. The effect of time on the weathering of silicate minerals: Why do weathering rates differ in the laboratory and field? Chem. Geol. **202**: 479–506. doi:10.1016/j.chemgeo.2003.03.001

Zapata, A., C. A. Rivera-Rondón, D. Valoyes, C. L. Muñoz-López, M. Mejía-Rocha, and J. Catalan. 2021. Páramo lakes of Colombia: An overview of their geographical distribution and physicochemical characteristics. Water **13**: 2175. doi:10.3390/w13162175

Acknowledgments

This research was conducted in the context of the Project "Análisis de la variación temporal de las características físico-químicas y biológicas de los lagos del Parque Nacional Cajas (PNC)" financed by the Research Directorate (DIUC) of the University of Cuenca, Ecuador, and the Municipal Public Enterprise of Telecommunications, Drinking Water, Sewerage and Sanitation of Cuenca, Ecuador (ETAPA EP). J.C. contribution was funded by the Spanish Government research grand "Alkaldia, PID2019-111137GB-C21, Ministerio de Ciencia y Tecnología." Chemical analyses were performed in the Environmental Laboratories, ETAPA EP, Ecuador. The authors thank Julissa Lucero from the Subgerencia de Gestión Ambiental ETAPA EP, for her assistance in the development of the land cover digital map used in this study. Research permissions in the Cajas NP by ETAPA EP and Ministerio del Ambiente, Agua y Transición Ecológica (MATEE) are acknowledged (ETAPA 003_SGA_2015_PNC_BD_VA_Hampel, MAE-DPACÑ-2015-0243, 189-2018-DPAA/MA, and 217-2020-DPAA/MA).

Submitted 13 August 2021
Revised 04 February 2022
Accepted 28 April 2022

Associate editor: John M. Melack